Electronic CD Study of a Helical Peptide Incorporating *Z*-Dehydrophenylalanine Residues: Conformation Dependence of the Simulated CD Spectra

Hisatoshi Komori and Yoshihito Inai*

Department of Environmental Technology and Urban Planning, Shikumi College, Graduate School of Engineering, Nagoya Institute of Technology, Gokiso-cho, Showa-ku, Nagoya 466-8555, Japan

Received: November 9, 2005; In Final Form: April 12, 2006

Electronic circular dichroism (CD) spectra as well as transitions from ground to excited states were predicted for a helical nonapeptide based on alternative sequence −[*Z*-α,*β*-dehydrophenylalanine (Δ^ZPhe)-X]− through semiempirical molecular orbital computation combined with time-dependent (TD) method. The simulation was performed for its various conformers that differ in helix type, helix sense, and Δ^ZPhe side-chain orientation. These conformational variations have been shown to depend largely on its CD spectra. Comparison between simulated and observed CD profiles reveals that peptide **1** in solution favors a right-handed 3_{10}-helix that adopts phenyl (Δ^ZPhe) planes basically in a vertical orientation with respect to the helix axis. These predictions were essentially supported from CD simulation of a shorter helical analogue at ab inito or density functional TD levels. The theoretical CD−conformation relationship should provide us useful guideline for determination of helix sense in the dehydropeptide, and for estimation of its conformations statistically averaged in solution.

Introduction

Circular dichroism (CD) spectroscopy provides us a quick overview about average conformations of a biological asymmetric chain without fine procedures.[1−6] Thus CD study has prevailed as one of the most fundamental structure analyses in bio-related science. In contrast to the experimentally convenient methodology, interpretation of CD profiles for chiral structures is not straightforward.[3] It requires theoretically precise evaluation of chiroptical parameters combined with excited states for possible conformers of a target chiral molecule.[3−5] As for protein segments or synthetic polypeptides, their theoretical CD simulations in the UV region were demonstrated to offer a successful guideline for the identification of a secondary structure.[5]

Peptide sequence introducing *Z*-α,*β*-dehydrophenylalanine (Δ^ZPhe) residues not only attracts biological interests[7] but also increasingly aims at the de novo designs of helix-based molecular backbones.[8,9] A peptide containing achiral Δ^ZPhe residues often tends to permit both left-handed and right-handed helices, accompanied with increasing composition of the achiral residue in a given sequence.[8b,h,i,9] Absolute identification of the preferential helix sense has been usually achieved on the basis of its electronic CD spectral profile around 280 nm (band I) assigned to Δ^ZPhe residue.[8b,g,h,9,10] The transition moment has been identified as charge transfer between phenyl and carbonyl groups, being approximately estimated as location of a phenyl−carbonyl line.[10a,b,d] The split CD profile has been simply interpreted on the basis of a spatial twist of the Δ^ZPhe transition moments (band I) along the backbone (e.g., the exciton chirality method).[8b,g,h,9−11]

On the other hand, strict theoretical interpretation of the chiroptical properties of unsaturated or unsaturated/saturated peptides containing Δ^ZPhe residues becomes more complicated than the case of peptides coded with saturated backbone sequences, which were employed for the pioneering electronic-CD simulations.[5] This reason is that each torsion angle around the phenyl−C^{β}═C^{α}−amide linkages influences the coplanarity between the side chain and backbone. As a result, excited states of Δ^ZPhe-containing peptides should depend on conformational variation located at or around the Δ^ZPhe residue, as seen in other conjugated molecular frameworks.[3a] The conformation-dependent nature will obstruct our approaches to the precise answer to how the main-chain and side-chain torsional variations in a helical Δ^ZPhe-containing peptide reflect the resulting CD spectra. This solution should require theoretical chiroptical parameters derived from molecular orbital (MO) computation of a whole peptide molecule with reference to its various conformers.

We here have attempted to simulate electronic CD spectra of a helical peptide incorporating Δ^ZPhe residues by means of MO calculation. The purpose for this simulation is to provide theoretical correlation between conformation and CD profile in a given dehydropeptide, as well as to confirm absolute determination of its helix sense. In the viewpoint of theoretical CD study, Δ^ZPhe-containing peptides are also regarded as a challenging framework in that torsional variations in the Δ^Z-Phe side chain (phenyl) and main chain (amide) should uniquely reflect electronic transition parameters.

Nonapeptide **1**, H-*β*-Ala-Δ^ZPhe-Aib-Δ^ZPhe-L-Phe-(Δ^ZPhe-Aib)$_2$-OCH_3 (*β*-Ala = *β*-alanine; Aib = α-aminoisobutyric acid),[9a] was mainly employed for the target dehydropeptide, which was shown to adopt a 3_{10}-helical conformation[12] essentially. Eight types of helical conformations for the present CD simulation were generated on the basis of helix sense (right-handedness or left-handedness), helix type (3_{10}-helix or α-helix), and side-chain orientation (vertical or parallel). The last term means that most of the Δ^ZPhe phenyl planes are arranged essentially in vertical (*v*) or parallel (*p*) orientations with respect to the helix axis (see Figure 1).

Recent advances in time-dependent (TD) ab initio or TD density functional theory (TD-HF or TD-DFT) successfully predict CD spectra for relatively small molecules.[3,4a,b,h−l] On

* Corresponding author. E-mail: inai.yoshihito@nitech.ac.jp.

10.1021/jp056501u CCC: $33.50
Published on Web 07/01/2006

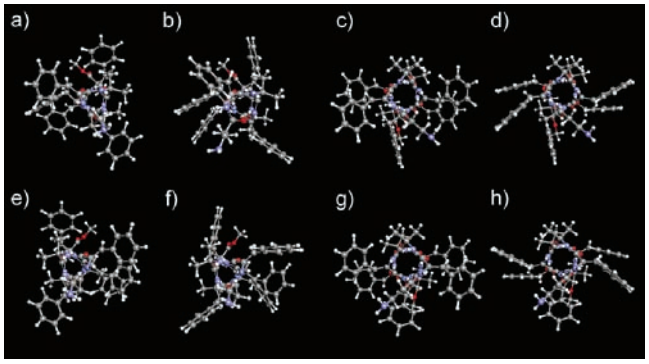

Figure 1. Peptide **1** in helical conformations: energy-minimized right-handed 3_{10}-helix with *v*-type (a) and *p*-type (b); right-handed α-helix with *v*-type (c) and *p*-type (d); energy-minimized left-handed 3_{10}-helix with *v*-type (e) and *p*-type (f); left-handed α-helix with *v*-type (g) and *p*-type (h). Each α-helix [(c), (d), (g), (h)] was made from the corresponding 3_{10}-helix [(a), (b), (e), (f)]: see the Experimental Section. Each conformer is viewed from the N-terminus.

the other hand, such advanced calculation will exact a high cost for the present molecular size with an adequate number of transition states. Thus, combination of semiempirical ZINDO/S-MO and TD method[4d−f,13−15] has been employed here to predict low-energy transition states involving oscillator strength (*f*) and rotatory strength (*R*) for each helical conformation: for simulation of transition states or chiroptical properties by semiemprical MO method, see refs 4d−f and 13−15. TD-HF or TD-DFT computations[13] have been also applied to a shorter analogue, CH_3CO-(Aib-Δ^ZPhe)$_2$-$NHCH_3$ (**2**). Consequently, conformational variations, especially in Δ^ZPhe side-chain orientations, depend largely on the transition states and CD profiles. The predicted CD−conformation correlation will offer us valuable information about the average population of such a dehydropeptide structure.

Experimental Section

Calculation Procedure. To simulate CD spectra of peptide **1**, several helical conformers were generated from a 3_{10}-helix through its energy minimization by the AM1-method in MOPAC97,[16] or subsequent modeling with torsion angles. Our present study does not intend to seek a global minimal conformation only through theoretical basis,[17,18] not dealing with other elegant methods.[19]

Although energy minimization of peptide **1** was already done,[9a] a similar calculation was again performed for several initial conformers as follows. Torsion angles adopted in ref 9b are basically used. That is, the segment of −Δ^ZPhe(2)-Aib(3)-Δ^ZPhe(4)-Phe(5)-Δ^ZPhe(6)-Aib(7)-Δ^ZPhe(8)− took a right-handed 3_{10}-helix [(ϕ, ψ, ω) = (−60°, −30°, 180°)].[20] Here (ϕ, ψ, ω) of the C-terminal Aib(9)-OCH_3 adopted (60°, 30°, 180°) as such helix inversion is often observed in similar sequences or Aib-containing sequences.[21] The β-Ala(1) residue took a trans form characterized by (θ, ψ, ω) = (180°, 180°, 180°).[22] All four χ^2(Δ^ZPhe) angles uniformly adopted 40° (*p*-type) or 140° (*v*-type),[23] whereas the side-chain orientations of Phe residue (χ^1, χ^2) were based on ref 24. The energy minimization was carried out as the variables of all bond lengths, bond angles, and torsion angles, together with a MOPAC97 keyword of MMOK for correction of amide-bond barrier.[16b,c] Among these conformers energy-minimized, a stable right-handed 3_{10}-helix was picked up for each of *v*-type (a) and *p*-type (b) (Figure 1a,b, respectively).

A similar optimization was performed for left-handed 3_{10}-helices where the seven residues of Δ^ZPhe(2) to Δ^ZPhe(8) were set to (60°, 30°) and the Aib(9) residue to (−60°, −30°).[20,21] The energy-minimized left-handed 3_{10}-helices with *v*-type (e) and *p*-type (f) are drawn in Figure 1e,f. In these 3_{10}-helices, [ϕ, ψ, ω, χ^2(Δ^ZPhe)] averaged for the seven residues of −Δ^ZPhe-Aib-Δ^ZPhe-Phe-Δ^ZPhe-Aib-Δ^ZPhe− is (a) (−40°, −40°, 179°, 136°), (b) (−43°, −45°, −179°, 53°), (e) (40°, 40°, −179°, 47°), and (f) (43°, 37°, 180°, 127°). [In (b), the average ψ is −36° if $\psi(2) = -98°$ is excepted.]

The rotation of the backbones [(a) and (b)] to an α-helical one [(ϕ, ψ, ω) = (−57°, −47°, 180°)],[22c,25] with retention of the side-chain orientations, yielded the corresponding right-handed α-helices [(c) and (d), respectively] (Figure 1c,d), whereas the backbones [(e) and (f)] changed to (57°, 47°, 180°)[22c,25] to yield the left-handed α-helices [(g) and (h), respectively] (Figure 1g,h). In (c)−(d) and (g)−(h), the Aib(9) residue took the opposite α-helix [(57°, 47°, 180°) or (−57°, −47°, 180°)], whereas the β-Ala residue was set to a trans form (180°, 180°, 180°). A similar manner was applied to the modeling of other helical conformations shown later, whereas each main chain of the Aib(9) takes the same sense as that of the preceding segment. The molecular graphics in this paper were basically drawn with the *ArgusLab* software.[15]

The electronic-transition and chiroptical parameters for each helical conformer were computed by combination of the time-dependent SCF-MO method with the ZINDO/S method[4d−f,13−15] in Gaussian 03, revision C.02,[13] with keywords "zindo=(nstates=160) td"[13] to yield low-energy 160 transition states involving oscillator strength (*f*) and rotatory strength (*R*). (For prediction of excited states or chiroptical properties by semiempirical MO method, see also refs 4d−f, 14, and 15).

R and *f* values are given in length-based and velocity-based forms on Gaussian 03.[13] We here have usually chosen CD profiles based on the velocity form that has an origin-independent nature in contrast to the origin-dependent length form.[3,4] Meanwhile, spectra in the length form are given for selected spectra in the velocity form.

TD-HF and TD-DFT-based simulations were also performed on Gaussian 03[13] for peptide **2** that was energy-minimized upon the AM1/MOPAC97[16] from a right-handed 3_{10}-helix with *v*-type or *p*-type side chain. "HF/6-31G**" and "B3LYP/6-31G**" levels[13,26] were chosen together with estimations of low-energy 20 transition states. A similar computation of "B3LYP/6-31G**" was performed for α-helical backbone (−57°, −47°, 180°)[22c,25] obtained through modeling of the energy-minimized 3_{10}-helix.

In all cases, a Gaussian-type function[27] based on wavelength was assumed to shape the CD spectra from *R* values and their positions, where a half Gaussian (1/e)-bandwidth (Δ/2) was assumed to be 14 nm.[27] In simulated and observed CD spectra, the $\Delta\epsilon$ value was expressed in terms of the Δ^ZPhe residue in the peptide sequence. Some simulated spectra gave the corresponding *R* [cgs (10^{-40} (erg esu cm)/Gauss)][13] and *f* values, both of which were expressed in terms of the peptide molecule.

Spectroscopic Measurement. CD and UV absorption data were obtained at ambient temperature on JASCO J-820 and V-550 spectrometers, respectively. CD spectra were mathematically smoothed to reduce noise. Molar extinction coefficients (ϵ) of peptide **1** as well as its Leu-analogue, H-β-Ala-Δ^ZPhe-Aib-Δ^ZPhe-L-Leu-(Δ^ZPhe-Aib)$_2$-OCH_3 (**3**),[9a] were also evaluated.

Results and Discussion

Conformational Dependence of Theoretical CD Spectra of Peptide 1. Figure 2 graphically summarizes velocity-based

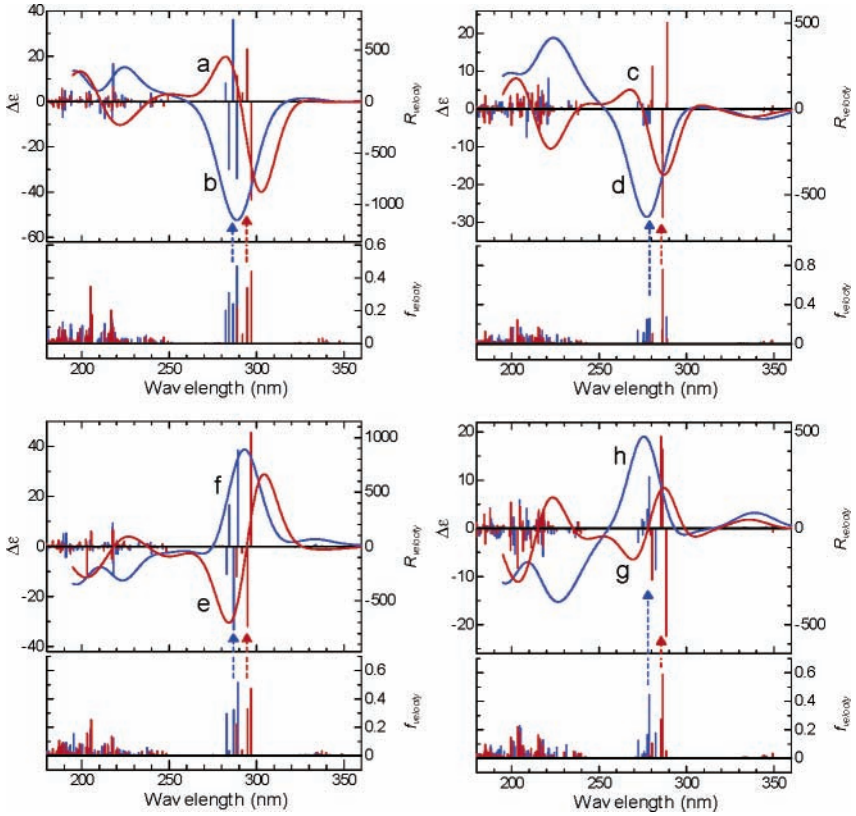

Figure 2. Excited-state parameters and CD spectra simulated for peptide **1** in several helical backbones with Δ^ZPhe side-chain orientations of *υ*-type (red) and *p*-type (blue): right-handed 3_{10}-helix [(a), (b)]; right-handed α-helix [(c), (d)]; left-handed 3_{10}-helix [(e), (f)]; left-handed α-helix [(g), (h)]. These conformations (a)−(h) correspond to those in Figure 1. The *f* and *R* values are predicted at the TD-ZINDO/S level in velocity form. Each arrow indicates the λ_{fmax} position at the band I for each structure. For the details, see the text.

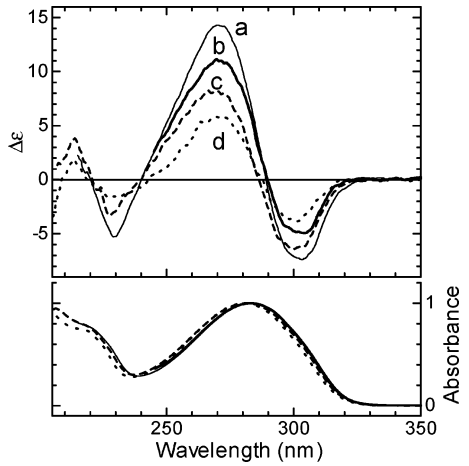

Figure 3. Experimental CD (top) and UV absorption spectra of peptide **1** at ambient temperature: [**1**] ([Δ^ZPhe]/4) = (a) ca. 5.4 mM and (b) 14 μM in chloroform; (c) 0.13 mM in tetrahydrofuran; (d) 0.13 mM in methanol. $\Delta\epsilon$ is expressed per concentration of Δ^ZPhe residue, and absorbance is expressed by normalization to unity at band I. For ϵ_{max} value in these solvents, see ref 33.

R and *f* values for the eight helical conformers shown in Figure 1. (For the corresponding length-based spectra, see SFigure 3. Comparison in velocity- and length-based simulations will be discussed later.) Interestingly, these conformational differences in helix sense, helix type, and Δ^ZPhe side chain produce a variety of excited states. For instance, right-handed 3_{10}-helices with the *υ*-type (a) and *p*-type (b) show clear *f* values around 280−300 nm, of which the transition states should be assigned to an experimental absorption band around 280 nm (band I), commonly observed for Δ^ZPhe-containing peptides.[8b,g,h,9,10]

Although small *f* signals appear above ca. 320 nm, these can be discriminated from signals that should be assigned to band I, on the basis of intensity and position in *f*. Our discussion hereafter focuses mainly on *R* values and CD profiles for the band I. The λ_{fmax} value for band I was also defined as the maximal position in the UV pattern at band I.[27] The CD spectrum at band I, based on its shape and λ_{fmax} position, is visually judged as split, nonsplit, or other patterns. (For the relationship in UV absorption maxima and CD profiles, see ref 11b.)

The λ_{fmax} of the *υ*-type appears at wavelengths somewhat longer (by ca. 10 nm) than that of the *p*-type. The corresponding four *R* values, in their signs and intensities, show remarkable differences between the two orientations. That is, the *υ*-type possesses a large negative *R* value at longer wavelengths of band I, and middle or small positive values at shorter wavelengths, whereas the *p*-type has alternate signs [(−)/(+)/(−)/(+) for longer to shorter wavelengths]. Correspondingly, CD profiles shaped with Gaussian functions for each *R* value produce dramatic difference. The *υ*-type outputs a split pattern of negative to positive peaks [(−)/(+)], as often observed for the alternative sequences −(Δ^ZPhe-X)− in a right-handed 3_{10}-helix,[8b,g,h,9,10b] whereas a nonsplit negative band is substantially seen for the *p*-type. Surprisingly, the Δ^ZPhe side-chain orientation merely can invert CD signs around 280 nm, although both backbones retain right-handed 3_{10}-helices offering a similar Δ^Z-Phe−Δ^ZPhe twist, which might promise the same split CD sign according to the exciton chirality method.[11] The phenomenon that dissimilar orientations of aromatic side chains lead to different chiroptical properties is experimentally or theoretically proposed for the unique helical polymer.[5d−g,28]

Although the number of transition states above ca. 260 nm is relatively limited, numerous transition states appear below ca. 250 nm in a complicated manner. The diversity should originate from coexistence of amide, Δ^ZPhe, and Phe chromophores.[5d,10] It has already been pointed out that Δ^ZPhe-based transition at this region disturbs general CD analysis in amide regions.[10] Meanwhile, theoretical CD spectra around 250−190 nm show relatively simple patterns. Conformer (a) seems to yield a split with negative signals at longer wavelengths, whereas two positive signals appear in the (b). In addition, dissimilar CD patterns are produced when the four Δ^ZPhe residues in conformer (a) of peptide **1** are replaced by Aib to give H-Aib$_4$-L-Phe-Aib$_4$-OCH$_3$ (**4**) and H-Aib$_4$-L-Ala-Aib$_4$-OCH$_3$ (**5**).[29−31] Thus the CD simulation at shorter wavelengths might offer us additional clues to the identification of peptide **1** conformation.

To highlight the helix type, CD spectra simulated for a right-handed α-helix[22c,25] are displayed in Figure 2c,d. Two side-chain orientations, *v*-type (c) and *p*-type (d), were taken from conformers (a) and (b), respectively. Conformer (c) yields three distinct *R* values at band I, characterized by signs of [(+)/(−)/(+)], to produce an incomplete split pattern at band I, in which the λ_{fmax} is close to the peak position in the negative CD band. In contrast, conformer (d) shows considerably smaller *R* values mainly with negative signs at band I to lead to a negative CD band. Consequently, the right-handed α-helix, whatever the *v*-type (c) or *p*-type (d), does not produce clear split-CD patterns at band I. In addition, CD spectra dissimilar in the *v*-type and *p*-type imply that the Δ^ZPhe side-chain orientation critically affects the CD spectra at band I.

Concerning the helix sense, CD spectra calculated for the left-handed 3$_{10}$-helices [(e), (f)] and α-helices [(g), (h)] are also shown in Figure 2, where each helix adopts two types of Δ^Z-Phe side-chain orientations noticed above. As expected, these CD signs are opposite to those of the corresponding right-handed helices [(a)−(d)]. The relations between CD spectral sign and helix sense should support our previous assignment[9] based on the exciton chirality method.[11] A similar tendency is seen in other 3$_{10}$- or α-helical backbones generated from the above 3$_{10}$-helices (SFigures 8−13).[32] These 3$_{10}$-helices yield essentially a split pattern for *v*-type orientation, or nonsplit for *p*-type (SFigures 8−11). Meanwhile, the α-helices give an incomplete split for *v*-type or nonsplit for *p*-type (SFigures 12 and 13).

Comparison with Experimental CD Spectra. CD spectra of peptide **1** in three kinds of solvents indicate a split-CD pattern around 280−285 nm (Figure 3).[33] In chloroform, the existence of a 3$_{10}$-helix was proposed from qualitative NMR and IR studies.[8a] Similarity in these CD spectral patterns suggests that a similar helix is present in methanol and tetrahydrofuran. Whereas the CD amplitude in chloroform is somewhat concentration-dependent, the split pattern is retained in (a) and (b). Comparison between Figures 2 (or SFigures 8−13) and 3 demonstrates that experimental CD profiles around 280 nm agree well with the theoretical one of a right-handed 3$_{10}$-helix combined with the *v*-type side-chain orientations (e.g., Figure 1a). An apparent split-CD pattern below ca. 250 nm in the simulated spectrum (Figure 2a) is also found in the experimental spectra in methanol and in tetrahydrofuran. This split pattern should originate from incorporation of Δ^ZPhe residues.[29−31]

Consequently, a right-handed 3$_{10}$-helix with the *v*-type orientations should be the most probable conformation among the eight-types of species. The theoretical prediction of a 3$_{10}$-helical backbone is supported by our previous NMR study of peptide **1** as well as by the preference for a 3$_{10}$-helix in analogous sequences.[9,18] A right-handed screw sense predicted

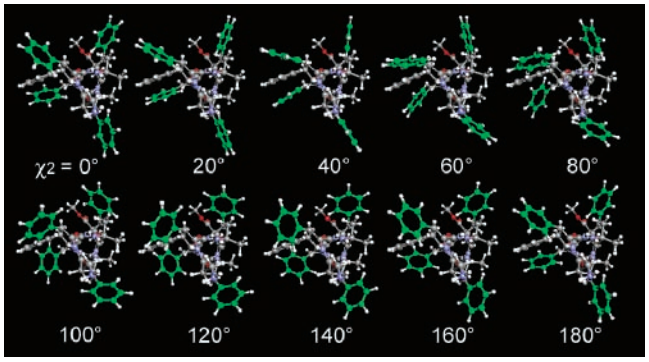

Figure 4. Right-handed 3$_{10}$-helices of peptide **1** with χ^2(Δ^ZPhe) angles ranging from 0 to 180°: the four phenyl rings of Δ^ZPhe are illustrated in green for clarification. Views from the N-terminus are shown.

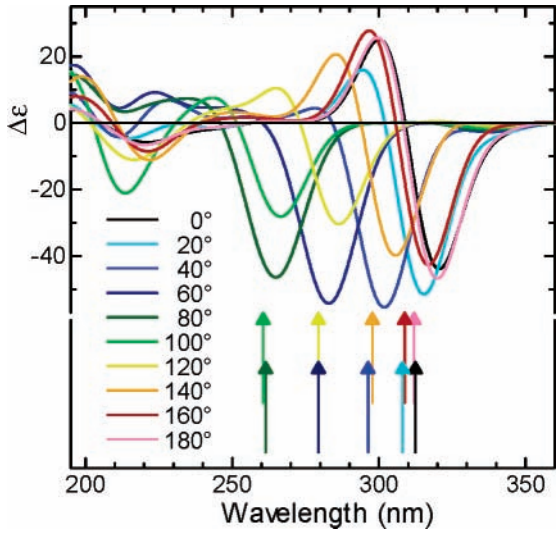

Figure 5. χ^2 dependence of CD spectra simulated for peptide **1** in right-handed 3$_{10}$-helices displayed in Figure 4. Each arrow indicates the corresponding λ_{fmax} position for each spectrum. The arrow at the shortest wavelength corresponds to $\chi^2 = 100°$.

is also consistent with that expected for peptide **1** sequence incorporating the internal L-residue that generally favors right-handedness.[12,24,34] Moreover, the *v*-type orientations in a 3$_{10}$-helix are found in the crystal structure of an analogous nonapeptide.[18]

Influence of Δ^ZPhe Side-Chain Orientation on Theoretical CD Spectra. In the preceding sections, Δ^ZPhe side-chain conformations largely influence theoretical CD profiles, beyond our expectations. To clarify the comprehensive side-chain effect, CD spectra of peptide **1** were simulated when the four χ^2(Δ^Z-Phe) angles in the right-handed 3$_{10}$-helix with the *v*-type (Figure 1a) simultaneously adopt 0° to 180° with a step of 20° (Figures 4 and 5). At each χ^2-point, all bond lengths and bond angles were re-optimized by the AM1 method.[16,35] Their CD patterns at band I are categorized into two types: i.e., the split of [(−)/(+)] sign, and the negative nonsplit. However, the opposite split is not substantially produced at band I, because a large negative *R* value is commonly found at longer wavelengths than the λ_{fmax} position. Correspondingly, when peptide **1** retains a 3$_{10}$-helix, the split CD spectra of [(−)/(+)] can be assigned to right-handed screw sense, being consistent with the previous assignment.[9] A definite split-type CD pattern at band I is seen in $\chi^2 = 0°$, 20°, 120°, 140°, 160°, and 180°, which visually corresponds to the *v*-type arrangement except for $\chi^2 = 20°$.

χ^2 of 20° appears to be in the *p*-type orientation, which is similar to $\chi^2 = 60°$. Nevertheless, the two χ^2 orientations

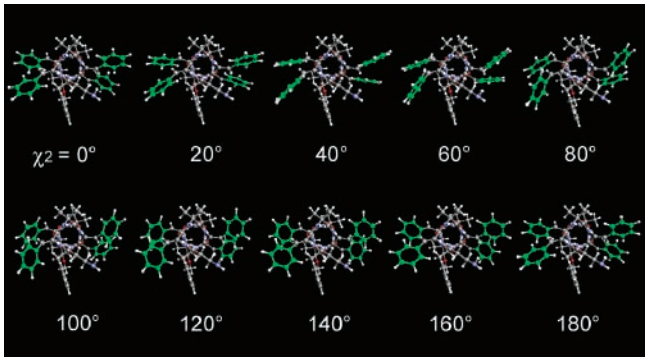

Figure 6. Right-handed α-helices of peptide **1** with χ^2(Δ^ZPhe) angles ranging from 0 to 180°: the four phenyl rings of Δ^ZPhe are illustrated in green for clarification. Views from the N-terminus are shown.

produce remarkably different CD patterns. A similar situation occurs in $\chi^2 = 100°$ and 140°. Thus the interpretation of CD spectra only from the phenyl orientation with respect to helix axis might be roughly treated. Strictly speaking, the excited-state and chiroptical properties should be dependent on both *local torsions* and *conformational asymmetry*. Regarding the λ_{fmax} position, the local coplanarity in the phenyl and $C^{\alpha}{=}C^{\beta}$ double bond is predominant. Increasing the coplanarity (χ^2 close to 0° or 180°) enlarges the π-conjugation system to result in a λ_{fmax} shift to longer wavelength, whereas the reduced coplanarity (χ^2 close to 90°) shifts λ_{fmax} to a shorter wavelength. As for the degree in coplanarity, $\chi^2 = 20°$ in question has higher coplanarity than 60°, whereas $\chi^2 = 100°$ has lower coplanarity than 140°. These differences in the coplanarity should influence chiroptical parameters associated with excited-state properties as presented in Figure 5. On the other hand, $\chi^2 = 40°$ and 140°, though showing similarity in coplanarity and λ_{fmax} position, produce nonsplit- and split-CD patterns, respectively. Here spatial asymmetry in the four phenyl orientations and the right-handed helical backbone should generate the remarkable changes in CD profiles. Although the *υ*- and *p*-based treatment used here supports intuitive understanding of structure−CD relation, more detailed description as discussed above should be required for fully consistent interpretation.

Because helical dehydropeptides in the crystal states often permit various χ^2(Δ^ZPhe) angles,[8a,c−f,h,i,18,21a] rotational motion about the single $C^{\beta}-C^{\gamma}$ bond might not be strictly restricted also in solution. In addition, the energy barrier around the χ^2 angle of a Δ^ZPhe residue involved in a 3_{10}-helical segment is predicted not to be very high.[36] Despite the theoretical side-chain effects, most of the actual CD spectra of peptide **1** as well as 3_{10}-helical sequences based on (Δ^ZPhe-X) units yield a clearly-split pattern at band I.[8b,9,10b] Accordingly, the Δ^ZPhe side-chain orientation should be dealt with as a statistical problem in CD spectra. The present CD simulation suggests that the *υ*-type orientations should be regarded as the probable population averaged in solution.

A similar χ^2 dependence was investigated for the right-handed α-helical conformation (Figure 1c) in $\chi^2 = 0-180°$ (at each χ^2-point, all bond lengths and bond angles were re-optimized). These orientations and CD spectra are illustrated in Figures 6 and 7, respectively. The side-chain rotation produces various CD spectra at band I, which are substantially classified into three patterns: a multi-split pattern of [(+)/(−)/(+)], a split pattern of [(+)/(−)], and a nonsplit negative band.

Among two split patterns ($\chi^2 = 100°$ and 120°), the λ_{fmax} for $\chi^2 = 100°$ is considerably shifted to a shorter wavelength. The other ($\chi^2 = 120°$) seems to have a considerably distorted split pattern, which, however, should be hidden by diverse CD

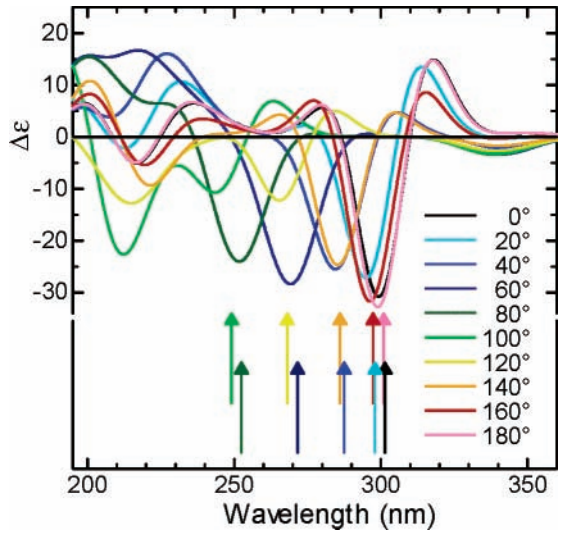

Figure 7. χ^2 dependence of CD spectra simulated for peptide **1** in right-handed α-helices displayed in Figure 6. Each arrow indicates the corresponding λ_{fmax} position for each spectrum. The arrow at the shortest wavelength corresponds to $\chi^2 = 100°$.

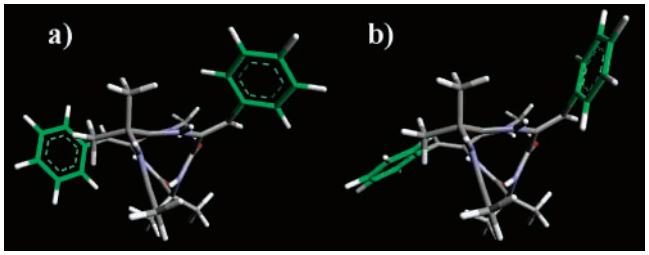

Figure 8. Views of peptide **2** in energy-minimized right-handed 3_{10}-helix with Δ^ZPhe side-chain orientations of (a) *υ*-type and (b) *p*-type.[9h,37]

patterns generated by statistical χ^2 rotation noticed above. In addition, the amide-region CD intensities (at ca. 200−250 nm) for $\chi^2 = 100°$ and 120° are comparable to those at band I unlike in Figure 2a,e. Therefore, an α-helical backbone in peptide **1** sequence will not tend to produce a split CD pattern at band I.

CD signs of peptide **1** are controllable by external chirality through the noncovalent chiral domino effect (NCDE).[9a] Boc-L-amino acid promotes the original split-CD amplitude at band I with retention of the split sign. Conversely, the corresponding D-isomer weakens the original amplitude or inverts the original signs. In the latter case, a split-CD profile with positive (for longer wavelength) to negative signs should be assigned to a left-handed 3_{10}-helix with the *υ*-type orientation. Thus, the inversion of split CD signs brings about the NCDE-mediated helix-to-helix inversion as proposed in ref 9a. The theoretical CD analysis enables us to determine absolutely the helix sense as a major population of conformation.

For additional information, the χ^2-rotation influences the position of λ_{fmax}, as indicated by arrows in Figures 5 and 7. As mentioned before, the λ_{fmax} value is being shifted to longer wavelength as the side-chain coplanarity increases (χ^2 close to 0°). Thus high frequency of χ^2-rotational motion might expand the spectral bandwidth.

TD-HF and TD-DFT Computations of a Shorter Peptide. Simulation at the semiempirical level should depend on the ZINDO/S-parametrization.[13,14] Meanwhile, as mentioned in the Introduction, ab initio or density functional levels for the current molecular size are hardly performed in our machine speculations. Instead, TD-HF (HF/6-31G**) and TD-DFT (B3LYP/6-31G**) computations[13] with a limited number of low-energy transition

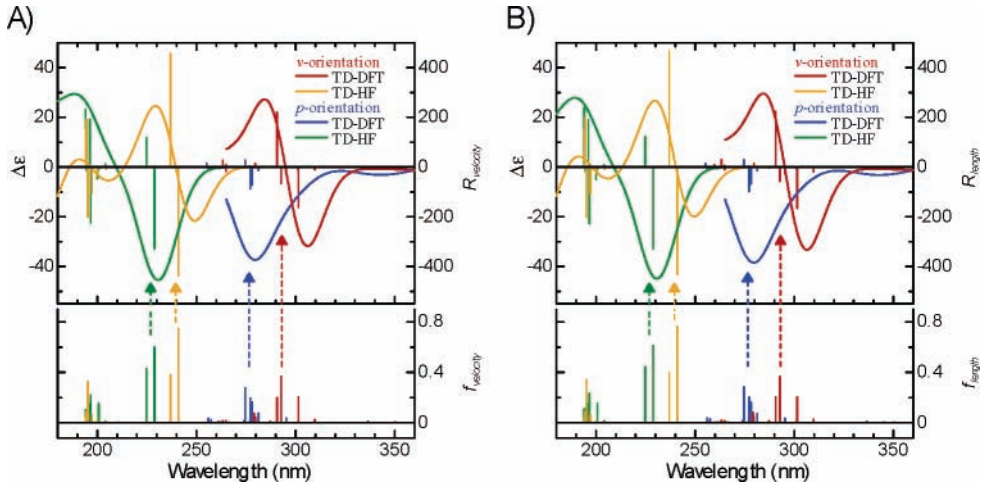

Figure 9. Excited-state parameters and CD spectra simulated for peptide **2** in the right-handed 3_{10}-helices with *υ*-type (Figure 8a) and *p*-type (Figure 8b) orientations by the TD-HF (HF/6-31G**) and TD-DFT (B3LYP/6-31G**) methods: based on the (A) velocity form and (B) length form.

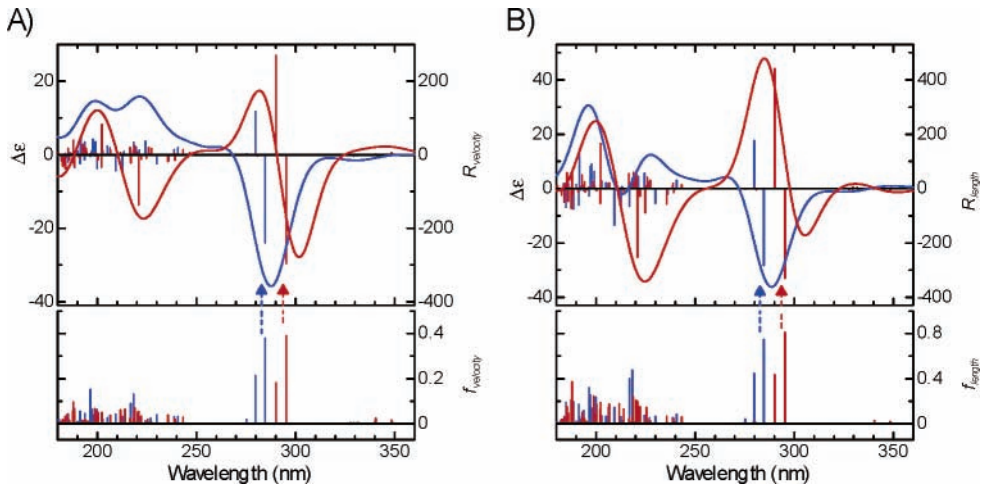

Figure 10. Excited-state parameters and CD spectra simulated for peptide **2** in the right-handed 3_{10}-helices with *υ*-type (Figure 8a) and *p*-type (Figure 8b) orientations by the TD-ZINDO/S method: based on the (A) velocity form and (B) length form. Red and blue lines correspond to *υ*-type and *p*-type, respectively.

states (20) were performed for a shorter analogue **2**,[37] which was energy-minimized from a right-handed 3_{10}-helix with the *υ*- or *p*-type through the AM1-method[16] (Figure 8).

CD patterns at band I are shown in Figure 9, where the transition states in the TD-HF appear at considerably shorter wavelengths.[38] The CD spectral difference between the velocity and length forms becomes smaller at the TD-HF and TD-DFT levels, compared with the case of the TD-ZINDO/S with 160 low-energy transition states (Figure 10), implying that the former two methods improve the reliability of the simulated CD results. In addition, the transition states in the TD-DFT are located at around 270−300 nm, close to the experimental positions.

A similar tendency is seen in the ZINDO/S- and DFT-based simulations for peptide **2** adopting an α-helix with *υ*- or *p*-type $[(\phi, \psi, \omega) = (-57°, -47°, 180°)]$[22c,25] (SFigures 14−16). That is, consistency in the velocity and length forms is more prominent in the TD-DFT-based CD spectra (SFigure 15), where the *υ*-type orientation produces a clearer split pattern of [(−)/(+)] at band I.

However, CD patterns at the three or two MO levels in the velocity form are similar to each other in that the *υ*-type yields a split CD pattern of (−) to (+), but the *p*-type gives a nonsplit, negative band. This implies that the preceding ZINDO/S-based results for peptide **1** play a satisfactory role for qualitative discussion.

Other Factors for Theoretical CD Spectra. Besides conformations, factors to influence theoretical CD spectra should be noted.

First, theoretical CD intensity depends largely on the (1/e)-bandwidth (Δ) of Gaussian function (for instance, SFigure 2), although the range of Δ value is less influential in the CD pattern.[27] In addition, the validity of the theoretical intensity should be referred to the experimental CD intensity, but we cannot estimate the experimental value precisely. Peptide **1** should permit a left-handed helix, thus preventing us from obtaining the experimental intensity of only right-handed helix. The coexistence of a left-handed helix is based on the fact that a larger CD intensity is observed for peptide **3** (SFigure 17) that substitutes L-Leu for the L-Phe of **1**, whereas both **1** and **3** adopt 3_{10}-helix and yield similar split CD pattern assigned to right-handed helix.[9a] That is, the content of the right-handed helical conformer should be higher in peptide **3**.[9a] Thus, a reasonable Δ value and experimental CD spectra of only the right-handed helix are required for the comparison of CD intensities.

Meanwhile, the effect of the Δ value has been briefly checked. If the experimental absorption profile of band I is assumed to be a Gaussian shape, (Δ/2) is estimated to be about 27 or 32 nm.[39] CD spectra of a right-handed 3_{10}-helix (Figure 1a) through these (Δ/2) values are given in SFigure 2. Although the profile retains a split pattern at band I, it becomes considerably dull.

To evaluate sharpness of the split shape, the difference ($\lambda_{12} = \lambda_1 - \lambda_2$) in the negative-peak position (λ_1) and the positive-peak position (λ_2) is used. The λ_{12} value is estimated to be 41 and 47 nm for ($\Delta/2$) = 27 and 32 nm, respectively, being considerably larger than λ_{12} (29−34 nm) observed in peptide **1** in tetrahydrofuran and chloroform.

Conversely, when the ($\Delta/2$) value to reproduce the experimental λ_{12} (29−34 nm) is used, the theoretical CD intensity at band I seems to be roughly similar to the experimental one of peptide **3** adopting predominantly a right-handed helix.[40] Thus, an appropriate choice of ($\Delta/2$) will reproduce experimental CD intensity. We here have usually used a smaller ($\Delta/2$) value, as mentioned in ref 27. The prediction that the Δ^ZPhe side-chain fluctuation generates diverse λ_{fmax} positions (Figures 5 and 7) allows us to consider that the broad absorption of band I is a consequence of integration of some individual conformers. In other words, the bandwidth for a single conformer might be more reduced. Correspondingly, a smaller ($\Delta/2$) value of 14 nm has been tentatively chosen to highlight CD spectral pattern at band I for each conformer.

Second, the difference between CD spectra in the velocity and length forms should be noted. In general, the velocity form is recommended due to its origin-independent nature, whereas the length form is origin-dependent.[3,4] Thus we have basically used the velocity form. As demonstrated in the short peptide **2**, the two forms yield similar transition parameters at the HF/6-31G** and B3LYP/6-31G** levels (Figure 9 and SFigure 15). In contrast, there appear to be some differences in the two results at the ZINDO/S level (Figure 10 and SFigure 16).

Also the length-based spectra of peptide **1** at the ZINDO/S-TD level are given for the corresponding velocity-based spectra: SFigure 3 (for Figure 2), SFigure 18A (for Figure 5), and SFigure 18B (for Figure 7). They are somewhat different from the corresponding velocity type. For instance, (i) intensities of *R* and *f* in the length seem to be basically larger than those in the velocity. (ii) In the χ^2 dependence of CD spectra of 3_{10}-helix, the tendency to split pattern at band I is stronger in the length. For instance, CD profiles for $\chi^2 = 40°$ and 100° appear as a nonsplit pattern in the velocity (Figure 5) but are regarded as split type in the length (SFigure 18A). (iii) Conversely, in the χ^2 dependence in an α-helix, the CD profile at band I in the length (SFigure 18B) appears essentially as the nonsplit or multi-split type, whereas $\chi^2 = 100°$ and 120° in the velocity seem to give the split-type (Figure 7). (iv) CD patterns of amide-based peptides show the difference in the two forms.[29] Despite the disagreements, the two forms lead to a similar relationship between the dehydropeptide conformation and CD pattern at band I.

Finally, all simulations for the transition states and CD spectra were performed without solvent effect. Solvent polarity (dielectric constant) is considered as an important factor in theoretical estimation of electronic excited properties.[41] Nevertheless, UV absorption and CD spectral patterns of peptides **1** and **3** in the three solvents having considerably different dielectric constants[13b] are essentially similar to each other (Figure 3 and SFigure 17). In the AM1-based energy-minimized dehydropeptide **1** or **2**, the TD-ZINDO/S or TD-DFT simulations without solvent effect produce marked oscillator strengths (*f*) around 270−300 nm (Figures 2a,b, 9, and 10, and SFigure 3a,b), reflecting the experimental position of band I in peptide **1** (Figure 3). Thus the solvent effect on these electronic parameters should be less significant in the present case.

Summary

The central topics in this paper are to estimate theoretical chiroptical parameters and their electronic CD spectra of a Δ^Z-Phe-containing helical peptide through MO computation dealing with its whole molecule. Simulated CD spectra of nonapeptide **1** characterized by alternative sequence −(Δ^ZPhe-X)− have been investigated in terms of its side-chain and main-chain conformations. The TD-ZINDO/S-based simulation has demonstrated that the CD profiles are sensitive to helix type (3_{10}- or α-helix), helix sense (right-handed or left-handed screw sense), and Δ^ZPhe side-chain orientation (*v*- or *p*-type). Comparison between theoretical and experimental CD profiles reveals that peptide **1** alone in solution adopts a right-handed 3_{10}-helical backbone with the *v*-type side-chain orientations as the average conformer. Our previous proposal of the NCDE-based helix-to-helix inversion[9a] has been also reconfirmed by the present simulations.

Whereas more precise evaluation will demand a TD-method at high MO levels, the present work signifies that conformation-dependent electronic CD profiles of the dehydropeptide have been qualitatively understood upon the TD-SCF computation of the whole molecule, without assumption of isolation of each Δ^ZPhe chromophore. The theoretical correlation between dehydropeptide conformations and the simulated CD profiles should be a promising indicator for experimental determination of statistically averaged conformers,[5] including absolute identification of helix sense, without intricate analyses. The reliability of the theoretical predictions will improve if additional conformational information (e.g., helix type) is provided in advance.

Acknowledgment. This work was partially supported by the project (No. 16550142) of the Ministry of Education, Culture, Sports, Science, and Technology of Japan. We sincerely thank the Editor-in-Chief and reviewers for providing valuable comments for the present paper.

Note Added in Proof. Our recent work of theoretical structural simulation[42] has also dealt with Δ^ZPhe side-chain conformers of another helical peptide in complex formation.

Supporting Information Available: Additional theoretical and experimental CD spectra, molecular graphics, and energy diagram. This material is available free of charge via the Internet at http://pubs.acs.org.

References and Notes

(1) For the principle of CD spectroscopy, see: (a) Schellman, J. A. *Chem. Rev.* **1975**, *75*, 323−331. (b) Sreerama, N.; Woody, R. W. *Methods Enzymol.* **2004**, *383*, 318−351.

(2) For elegant examples of biopolymers, see: (a) Sreerama, N.; Woody, R. W. *Protein Sci.* **2004**, *13*, 100−112. (b) Chin, D. H.; Woody, R. W.; Rohl, C. A.; Baldwin, R. L. *Proc. Natl. Acad. Sci. U.S.A.* **2002**, *99*, 15416−15421. (c) Cowman, M. K.; Fasman, G. D. *Proc. Natl. Acad. Sci. U.S.A.* **1978**, *75*, 4759−4763.

(3) (a) Furche, F.; Ahlrichs, R.; Wachsmann, C.; Weber, E.; Sobanski, A.; Vögtle, F.; Grimme, S. *J. Am. Chem. Soc.* **2000**, *122*, 1717−1724. (b) Autschbach, J.; Ziegler, T.; Gisbergen, S. J. A.; Baerends, E. J. *J. Chem. Phys.* **2002**, *116*, 6930−6940.

(4) (a) Stephens, P. J.; McCann, D. M.; Devlin, F. J.; Cheeseman, J. R.; Frisch, M. J. *J. Am. Chem. Soc.* **2004**, *126*, 7514−7521. (b) Diedrich, C.; Grimme, S. *J. Phys. Chem. A* **2003**, *107*, 2524−2539. (c) Brown, A.; Kemp, C. M.; Mason, S. F. *J. Chem. Soc.* **1971**, 751−755. (d) Telfer, S. G.; Tajima, N.; Kuroda, R. *J. Am. Chem. Soc.* **2004**, *126*, 1408−1418. (e) Ankai, E.; Sakakibara, K.; Uchida, S.; Uchida, Y.; Yokoyama, Y.; Yokoyama, Y. *Bull. Chem. Soc. Jpn.* **2001**, *74*, 1101−1108. (f) Kawai, M.; Nagai, U.; Inai, Y.; Yamamura, H.; Akasaka, R.; Takagi, S.; Miwa, Y.; Taga, T. *Biopolymers* **2005**, *80*, 186−198. (g) Shustov, G. V.; Kadorkina, G. K.; Kostyanovsky, R. G.; Rauk, A. *J. Am. Chem. Soc.* **1988**, *110*, 1719−1726. (h) Bouř, P. *J. Phys. Chem. A* **1999**, *103*, 5099−5104. (i) Fukuyama, T.; Matsuo, K.; Gekko, K. *J. Phys. Chem. A* **2005**, *109*, 6928−6933. (j)

Lebon, F.; Longhi, G.; Gangemi, F.; Abbate, S.; Priess, J.; Juza, M.; Bazzini, C.; Caronna, T.; Mele, A. *J. Phys. Chem. A* **2004**, *108*, 11752−11761. (k) Wan, J.; Xu, X.; Ren, Y.; Yang, G. *J. Phys. Chem. B* **2005**, *109*, 11088−11090. (l) Watanabe, M.; Suzuki, H.; Tanaka, Y.; Ishida, T.; Oshikawa, T.; Tori-i, A. *J. Org. Chem.* **2004**, *69*, 7794−7801.

(5) For leading studies of theoretical CD spectra of (poly)peptides in the UV region: (a) Manning M. C.; Woody, R. W. *Biopolymers* **1991**, *31*, 569−586. (b) Woody, R. W.; Koslowski, A. *Biophys. Chem.* **2002**, *101-102*, 535−551. (c) Sreerama, N.; Manning, M. C.; Powers, M. E.; Zhang, J.-X.; Goldenberg, D. P.; Woody, R. W. *Biochemistry* **1999**, *38*, 10814−10822. (d) Woody, R. W. *Biopolymers* **1972**, *11*, 1149−1171. See also ref 1b. For theoretical CD simulations of polypeptides carrying unusual aromatic side chains, see: (e) Sisido, M.; Egusa, S.; Imanishi, Y. *J. Am. Chem. Soc.* **1983**, *105*, 1041−1049. (f) Sisido, M.; Imanishi, Y. *Macromolecules* **1985**, *18*, 890−894. (g) Sisido, M.; Ishikawa, Y.; Harada, M.; Itoh, K. *Macromolecules* **1991**, *24*, 3999−4003.

(6) Although CD spectroscopy or its simulation in the infrared region have been effectively performed in chiral chemistry and biochemistry,[6a−j] the present paper focuses on electronic CD study in the UV region. For elegant methods and applications for vibrational spectroscopy, see: (a) Stephens, P. J. *J. Phys. Chem.* **1985**, *89*, 748−752. (b) Stephens, P. J.; Devlin, F. J. *Chirality* **2000**, *12*, 172−179. (c) Devlin, F. J.; Stephens, P. J.; Cheeseman, J. R.; Frisch, M. J. *J. Am. Chem. Soc.* **1996**, *118*, 6327−6328. (d) Bohr, H. G.; Frimand, K.; Jalkanen, K. J.; Nieminen, R. M.; Suhai, S. *Phys. Rev. E.* **2001**, *64*, 021905 (13 pages). (e) Bouř, P.; Keiderling, T. A. *J. Phys. Chem. B* **2005**, *109*, 23687−23697. (f) Bak, K. L.; Jørgensen, P.; Helgaker, T.; Ruud, K. Jensen, H. J. A. *J. Chem. Phys.* **1993**, *98*, 8873−8887. (g) Pancoska, P.; Bitto, E.; Janota, V.; Urbanova, M.; Gupta, V. P.; Keiderling, T. A. *Protein Sci.* **1995**, *4*, 1384−1401. (h) Schweitzer-Stenner, R.; Eker, F.; Griebenow, K.; Cao, X.; Nafie, L. A. *J. Am. Chem. Soc.* **2004**, *126*, 2768−2776. (i) McColl, I. H.; Blanch, E. W.; Hecht, L.; Barron, L. D. *J. Am. Chem. Soc.* **2004**, *126*, 8181−8188. (j) Birke, S. S.; Agbaje, I.; Diem, M. *Biochemistry* **1992**, *31*, 450−455. For comparisons between vibrational and electronic CDs, see ref 6g.

(7) (a) Shimohigashi, Y.; Kodama, H.; Imazu, S.; Horimoto, H.; Sakaguchi, K.; Waki M, Uchida, H.; Kondo, M.; Kato, T.; Izumiya, N. *FEBS Lett.* **1987**, *222*, 251−255. (b) Katsu, T.; Sanchika, K.; Takahashi, M.; Kishimoto, Y.; Fujita, Y.; Yoshitomi, H.; Waki, M.; Shimohigashi, Y. *Chem. Pharm. Bull.* **1990**, *38*, 2880−2881.

(8) (a) Ciajolo, M. R.; Tuzi, A.; Pratesi, C. R.; Fissi, A.; Pieroni, O. *Biopolymers* **1990**, *30*, 911−920. (b) Pieroni, O.; Fissi, A.; Pratesi, C.; Temussi, P. A.; Ciardelli, F. *J. Am. Chem. Soc.* **1991**, *113*, 6338−6340. (c) Jain, R.; Chauhan, V. S. *Biopolymers* **1996**, *40*, 105−119. (d) Ramagopal, U. A.; Ramakumar, S.; Sahal, D.; Chauhan, V. S. *Proc. Natl. Acad. Sci. U.S.A.* **2001**, *98*, 870−874. (e) Rajashankar, K. R.; Ramakumar, S.; Chauhan, V. S. *J. Am. Chem. Soc.* **1992**, *114*, 9225−9226. (f) Mitra, S. N.; Dey, S.; Karthikeyan, S.; Singh, T. P. *Biopolymers* **1997**, *41*, 97−105. (g) Guo, Y.-M.; Oike, H.; Aida, T. *J. Am. Chem. Soc.* **2004**, *126*, 716−717. (h) Tuzi, A.; Ciajolo, M. R.; Guarino, G.; Temussi, P. A.; Fissi, A.; Pieroni, O. *Biopolymers* **1993**, *33*, 1111−1121. (i) Ramagopal, U. A.; Ramakumar, S.; Mathur, P.; Joshi, R.; Chauhan, V. S. *Protein Eng.* **2002**, *15*, 331−335.

(9) (a) Inai, Y.; Komori, H. *Biomacromolecules* **2004**, *5*, 1231−1240. (b) Inai, Y.; Ousaka, N.; Okabe, T. *J. Am. Chem. Soc.* **2003**, *125*, 8151−8162. (c) Inai, Y.; Tagawa, K.; Takasu, A.; Hirabayashi, T.; Oshikawa, T.; Yamashita, M. *J. Am. Chem. Soc.* **2000**, *122*, 11731−11732. (d) Inai, Y.; Ishida, Y.; Tagawa, K.; Takasu, A.; Hirabayashi, T. *J. Am. Chem. Soc.* **2002**, *124*, 2466−2473. (e) Inai, Y.; Komori, H.; Takasu, A.; Hirabayashi, T. *Biomacromolecules* **2003**, *4*, 122−128. (f) Inai, Y.; Kurokawa, Y.; Kojima, N. *J. Chem. Soc., Perkin Trans. 2* **2002**, 1850−1857. (g) Inai, Y.; Kurokawa, Y.; Hirabayashi, T. *Biopolymers* **1999**, *49*, 551−564. (h) Inai, Y. *Recent Research Developments in Macromolecules*; Research Signpost: India, 2002; Chapter 2.

(10) (a) Pieroni, O.; Montagnoli, G.; Fissi, A.; Merlino, S.; Ciardelli, F. *J. Am. Chem. Soc.* **1975**, *97*, 6820−6826. (b) Pieroni, O.; Fissi, A.; Jain, R. M.; Chauhan, V. S. *Biopolymers* **1996**, *38*, 97−108. (c) Pieroni, O.; Fissi, A.; Merlino, S.; Ciardelli, F. *Isr. J. Chem.* **1977**, *15*, 22−28. (d) Inai, Y.; Ito, T.; Hirabayashi, T.; Yokota, K. *Biopolymers* **1993**, *33*, 1173−1184.

(11) For the exciton chirality method, see: (a) Harada, N.; Chen, S. L.; Nakanishi, K. *J. Am. Chem. Soc.* **1975**, *97*, 5345−5352. (b) Harada, N.; Nakanishi, K. *Circular Dichroic Spectroscopy. Exciton Coupling in Organic Stereochemistry*; University Science Books: Mill Valley, CA, 1983.

(12) For a 3_{10}-helix, see: (a) Barlow, D. J.; Thornton, J. M. *J. Mol. Biol.* **1988**, *201*, 601−619. (b) Toniolo, C.; Benedetti, E. *Trends Biochem. Sci.* **1991**, *16*, 350−353.

(13) (a) Frisch, M. J.; Trucks, G. W.; Schlegel, H. B.; Scuseria, G. E.; Robb, M. A.; Cheeseman, J. R.; Montgomery, J. A., Jr.; Vreven, T.; Kudin, K. N.; Burant, J. C.; Millam, J. M.; Iyengar, S. S.; Tomasi, J.; Barone, V.; Mennucci, B.; Cossi, M.; Scalmani, G.; Rega, N.; Petersson, G. A.; Nakatsuji, H.; Hada, M.; Ehara, M.; Toyota, K.; Fukuda, R.; Hasegawa, J.; Ishida, M.; Nakajima, T.; Honda, Y.; Kitao, O.; Nakai, H.; Klene, M.; Li, X.; Knox, J. E.; Hratchian, H. P.; Cross, J. B.; Bakken, V.; Adamo, C.; Jaramillo, J.; Gomperts, R.; Stratmann, R. E.; Yazyev, O.; Austin, A. J.; Cammi, R.; Pomelli, C.; Ochterski, J. W.; Ayala, P. Y.; Morokuma, K.; Voth, G. A.; Salvador, P.; Dannenberg, J. J.; Zakrzewski, V. G.; Dapprich, S.; Daniels, A. D.; Strain, M. C.; Farkas, O.; Malick, D. K.; Rabuck, A. D.; Raghavachari, K.; Foresman, J. B.; Ortiz, J. V.; Cui, Q.; Baboul, A. G.; Clifford, S.; Cioslowski, J.; Stefanov, B. B.; Liu, G.; Liashenko, A.; Piskorz, P.; Komaromi, I.; Martin, R. L.; Fox, D. J.; Keith, T.; Al-Laham, M. A.; Peng, C. Y.; Nanayakkara, A.; Challacombe, M.; Gill, P. M. W.; Johnson, B.; Chen, W.; Wong, M. W.; Gonzalez, C.; and Pople, J. A. *Gaussian 03*, revision C.02; Gaussian, Inc.: Wallingford, CT, 2004. For the manual including the full references, see also: (b) *The Official Gaussian Website* (http://www.Gaussian.com/).

(14) For the ZINDO/S method, see: (a) Zerner, M. C.; Loew, G. H.; Kirchner, R. F.; Mueller-Westerhoff, U. T. *J. Am. Chem. Soc.* **1980**, *102*, 589−599. (b) Ridley, J. E.; Zerner, M. C. *Theo. Chim. Acta* **1973**, *32*, 111−134. (c) Ridley, J. E.; Zerner, M. C. *Theo. Chim. Acta* **1976**, *42*, 223−236. (d) Thompson, M. A.; Zerner, M. C. *J. Am. Chem. Soc.* **1991**, *113*, 8210−8125. For the full references, see ref 13b.

(15) ZINDO-based chiroptical parameters can also be simulated in another software: see Thompson, M. A. *ArgusLab 4.0*; Planaria Software LLC: Seattle, WA, 2004 (http://www.arguslab.com). We here obtained these parameters by using Gaussian 03.[13]

(16) For the AM1 method, see: (a) Dewar, M. J. S.; Zoebisch, E. G.; Healy, E. F.; Stewart, J. J. P. *J. Am. Chem. Soc.* **1985**, *107*, 3902−3909. For MOPAC97, see: (b) Stewart, J. J. P. *MOPAC97*; Fujitsu Ltd.: Tokyo, Japan, 1998. (c) Stewart, J. J. P. *MOPAC 93 Manual*, revision number 2; Fujitsu Ltd.: Tokyo, Japan, 1993.

(17) We aim to correlate several helix-based conformers with their electronic CD patterns. The 3_{10}-helical structure of peptide **1** was proposed in our previous NMR spectroscopy in $CDCl_3$.[9a] In addition, an N-blocked nonapeptide with a similar sequence was found to adopt a typical 3_{10}-helical conformation in its crystal state.[18] Accordingly, 3_{10}-helices from the AM1-energy minimization were used for CD simulation, or for starting conformation to generate other conformations through variation in the torsion angles. All conformations generated have been used to obtain the conformation−electronic CD correlation. For the detailed procedures, see the text.

(18) Inai, Y.; Oshikawa, T.; Yamashita, M.; Tagawa, K.; Hirabayashi, T. *Biopolymers* **2003**, *70*, 310−322.

(19) For other semiempirical MO methods or their applications to peptide conformations (PM3,[19a−d] SCC-DFTB,[19c,e,f] or OM2[19d,g]), see: (a) Stewart, J. J. P. *J. Comput. Chem.* **1989**, *10*, 209−220. (b) Wu, Y.-D.; Zhao, Y.-L. *J. Am. Chem. Soc.* **2001**, *123*, 5313−5319. (c) Elstner, M.; Jalkanen, K. J.; Knapp-Mohammady, M.; Frauenheim, T.; Suhai, S. *Chem. Phys.* **2001**, *263*, 203−219. (d) Mohle, K.; Hofmann, H.-J.; Thiel, W. *J. Comput. Chem.* **2001**, *22*, 509−520. (e) Elstner, M.; Jalkanen, K. J.; Knapp-Mohammady, M.; Frauenheim, T.; Suhai, S. *Chem. Phys.* **2000**, *256*, 15−27. (f) Han, W.-G.; Elstner, M.; Jalkanen, K. J.; Frauenheim, T.; Suhai, S. *Int. J. Quantum Chem.* **2000**, *78*, 459−479. (g) Weber, W.; Thiel, W. *Theor. Chem. Acc.* **2000**, *103*, 495−506. For the AM1, see also refs 16 and 19c−e.

(20) (a) Paterson, Y.; Rumsey, S. M.; Benedetti, E.; Némethy, G.; Scheraga, H. A. *J. Am. Chem. Soc.* **1981**, *103*, 2947−2955. (b) Venkatachalam, C. M. *Biopolymers* **1968**, *6*, 1425−1436.

(21) (a) Inai, Y.; Oshikawa, T.; Yamashita, M.; Hirabayashi, T.; Ashitaka, S. *J. Chem. Soc., Perkin. Trans. 2* **2001**, 892−897. (b) Karle, I. L.; Flippen-Anderson, J. L.; Uma, K.; Balaram, H.; Balaram, P. *Proc. Natl. Acad. Sci. U.S.A.* **1989**, *86*, 765−769. (c) Toniolo, C.; Crisma, M.; Bonora, G. M.; Benedetti, E.; Di Blasio, B.; Pavone, V.; Pedone, C.; Santini, A. *Biopolymers* **1991**, *31*, 129−138. (d) Okuyama, K.; Ohuchi, S. *Biopolymers* **1996**, *40*, 85−103. For helix termini of more native sequences, see: (e) Schellman, C. In *Protein Folding*; Jaenicke, R., Ed.; Elsevier: North-Holland Biomedical, Amsterdam, 1980; pp 53−61. (f) Aurora, R.; Srinivasan, R.; Rose, G. D. *Science* **1994**, *264*, 1126−1130. (g) Sagermann, M.; Mårtensson, L.-G.; Baase, W. A.; Matthews, B. W. *Protein Sci.* **2002**, *11*, 516−521.

(22) For the definition of β-residue torsion angles, see: (a) Karle, I. L.; Pramanik, A.; Banerjee, A.; Bhattacharjya, S.; Balaram, P. *J. Am. Chem. Soc.* **1997**, *119*, 9087−9095. (b) Cheng, R. P.; Gellman, S. H.; DeGrado, W. F. *Chem. Rev.* **2001**, *101*, 3219−3232. The other torsion angles basically followed the standard definition: (c) IUPAC-IUB Commission on Biochemical Nomenclature. *Biochemistry* **1970**, *9*, 3471−3479. ψ and ω angles for C-terminal ester residue are defined for $N-C^{\alpha}-C-O-C(H_3)$, according to ref 22c. Meanwhile, the notation of $\chi^2(\Delta^Z\text{Phe}) \geq 0°$ is used in the present paper.

(23) The two χ^2-orientations were taken from ref 23a. Similar orientations are also estimated in Δ^ZPhe residue incorporated into a 3_{10}-helical chain through molecular mechanics.[23b−f] Likewise, the AM1-based computation predicts two local minima at $\chi^2 = 50$ and 140°, which will be shown in SFigure 1. For theoretical estimations of side-chain orientation (χ^2) of β-substituted α,β-dehydroresidues, see: (a) Ajò, D.; Casarin, M.; Granozzi, G. *J. Mol. Struct. (THEOCHEM)* **1982**, *86*, 297−300. (b) Inai, Y.; Oshikawa, T.; Yamashita, M.; Hirabayashi, T.; Kurokawa, Y. *Bull. Chem. Soc. Jpn.* **2001**, *74*, 959−966. (c) Inai, Y.; Hirabayashi, T. *Biopolymers* **2001**, *59*, 356−369. For parameters, program, and references for the mechanics, see refs 23d−f, and also refs 9a, 20a. (d) Momany, F. A.; McGuire, R. F.; Burgess, A. W.; Scheraga, H. A. *J. Phys. Chem.* **1975**,

79, 2361−2381. (e) Beppu, Y. *Comput. Chem.* **1989**, *13*, 101. (f) Sisido, M. *Peptide Chem.* **1992**, *1991*, 105−110.

(24) Zimmerman, S. S.; Pottle, M. S.; Némethy, G.; Scheraga, H. A. *Macromolecules* **1977**, *10*, 1−9.

(25) (a) Arnott, S.; Dover: S. D. *J. Mol. Biol.* **1967**, *30*, 209−212. (b) Arnott, S.; Wonacott, A. J. *J. Mol. Biol.* **1966**, *21*, 371−383.

(26) For examples of TD-HF and TD-DFT, see refs 3 and 4a,b,g,h. For the B3LYP method, see: (a) Stephens, P. J.; Devlin, F. J.; Chabalowski, C. F.; Frisch, M. J. *J. Phys. Chem.* **1994**, *98*, 11623−11627. (b) Becke, A. D. *J. Chem. Phys.* **1993**, *98*, 5648−5652. (c) Lee, C.; Yang, W.; Parr, R. G. *Phys. Rev. B.* **1998**, 37, 785−789.

(27) Gaussian-type functions based on wavenumber (energy) or wavelength are generally employed to simulate CD spectra: see refs 1 and 3−5. The (Δ/2) value being smaller than that estimated from its absorption profile is used to increase sensitivity of each transition state to CD spectra, because conformational variations (especially, χ^2-rotation) depend largely on λ-positions predicted as shown later. As pointed out in ref 5a, simulated CD spectra are sensitive to the (Δ/2) value. CD spectral profiles for qualitative discussion, despite the (Δ/2) dependence of CD intensities, should be essentially retained in a (Δ/2) range. For instance, see SFigure 2, which will be discussed later. In addition, the peak position at band I was estimated from a similar treatment in the corresponding $f-\lambda$ relationship: a Gaussian-type function based on wavelength with (Δ/2) = 14 nm was used to produce the UV absorption profile. In most cases, a strong band around 250−310 nm was assigned to the UV pattern at band I. For the experimental relation between the Gaussian-type absorption shape and f, see: (a) Rauch, C. J.; Heer, C. V. *Phys. Rev.* **1957**, *105*, 914−920.

(28) Tang, H.-Z.; Boyle, P. D.; Novak, B. M. *J. Am. Chem. Soc.* **2005**, *127*, 2136−2142.

(29) To estimate the influence of Δ^ZPhe or Phe chromophores on CD spectra in the amide region, the two peptides were generated from peptide **1** in helical conformations (Figure 1a,c). Here the four Δ^ZPhe residues were replaced by Aib residues, and furthermore the L-Phe residue is replaced by the L-Ala residue. After re-optimization of their bond lengths and bond angles through the AM1, peptides **4** and **5** in the right-handed 3_{10}-helix or α-helix were simulated to provide the CD spectra in the Supporting Information (SFigures 4−7).[30] On the whole, the velocity-based and length-based CD patterns show the difference. Especially, signals around 210−220 nm become positive in the velocity, but essentially negative in the length. This implies that it is a difficult problem to predict the amide-based CD spectra[31] through the present method, whereas it should be valid for strong discrete transitions such as band I. An inadequate choice of the bandwidth might be also related to the disagreement.[31] However, it is obvious that CD spectra of peptide **1** in the amide region are completely different from those of **4** and **5** lacking Δ^ZPhe (SFigures 4−7). Therefore, the incorporation of the Δ^ZPhe residue indeed influences the CD profile in the amide region, as pointed out.[10a,b,d]

(30) In the velocity form, the positive CD sign at 210−220 nm is not consistent with the experimental and theoretical standards of a right-handed 3_{10}- or α-helix.[5a,30a] On the other hand, similarity in the R patterns in the velocity and length forms (SFigures 4−7) suggests that some difference in relative intensity of $+R$ or $-R$ is considerably influential in the CD sign. Further investigations will be needed for CD simulation of amide-based peptides by the MO method. For experimental CD of 3_{10}-helix, see: (a) Toniolo, C.; Polese, A.; Formaggio, F.; Crisma, M.; Kamphuis, J. *J. Am. Chem. Soc.* **1996**, *118*, 2744−2745.

(31) Woody and co-workers successfully demonstrated CD spectra in the far-UV region.[5a−c] Here transition parameters of the monomer unit are individually evaluated for computation of rotatory strengths. Refinement of the bandwidth for specific transition states also yields good results for experimental CD spectra.[5a] Our CD simulation is generated by MO computations of the whole molecule, and the bandwidth of specific transition states is not refined here.

(32) The Supporting Information provides velocity-based CD spectra for the following helical backbones of (ϕ, ψ): for a 3_{10}-helix, (−44°, −33°)[32a] (SFigure 8A), (−53°, −36°)[32b] (SFigure 9A), (−60°, −30°)[20] (SFigure 10A), and (−71°, −18°)[12a] (SFigure 11A); for an α-helix, (−53°, −52°)[32c] (SFigure 12A), and (−63°, −42°)[12b,32d] (SFigure 13A). For the references of these backbones, see: (a) Malcolm, B. R.; Walkinshaw, M. D. *Biopolymers* **1986**, *25*, 607−625. (b) Hodgkin, E. E.; Clark, J. D.; Miller, K. R.; Marshall, G. R. *Biopolymers* **1990**, *30*, 533−546. (c) Leach, S. J.; Némethy, G.; Scheraga, H. A. *Biopolymers* **1966**, *4*, 887−904. (d) Blundell, T.; Barlow, D.; Borkakoti, N.; Thornton, J. *Nature* **1983**, *306*, 281−283. The original (ϕ, ψ) values[32a−c] are rounded off to integer (for the rounded values of refs 32a,c, see also ref 5a), and the (−53°, −36°) is noted as "3.6$_{10}$-helix" in ref 32b. CD spectra of the corresponding left-handed helices having the positive values of the above (ϕ, ψ) are also shown in SFigures 8B−13B, respectively. In all cases, the ω angle is set to 180°. The exciton chirality method[11] for similar helical sequences based on $-(\Delta^Z\text{Phe-X})_n-$ predicts a split-CD pattern of [(−)/(+)]:[9c,g,32e] (e) Inai, Y.; Sakakura, Y.; Hirabayashi, T. *Polym. J.* **1998**, *30*, 828−832. Manning and Woody elegantly demonstrated CD spectra in amide regions of various α- or 3_{10}-helical structures of polypeptides based on standard residues.[5a] For example of DFT-based simulation in oligopeptide, see also ref 4h.

(33) In chloroform, the difference in CD amplitude between (a) and (b) might be due to aggregation of peptide **1**. ϵ_{max} (per Δ^ZPhe residue around 280−285 nm) was estimated to be 1.8×10^4 (283−284 nm) in chloroform, 1.9×10^4 (282 nm) in tetrahydrofuran, and 1.9×10^4 (281 nm) in methanol. For peptide **3**, $\epsilon_{max} = 1.8 \times 10^4$ (283−284 nm) in chloroform, 1.8×10^4 (280−281 nm) in tetrahydrofuran, and 1.8×10^4 (279−281 nm) in methanol. A similar value in ϵ_{max} of the Δ^ZPhe residue was reported.[9b,10] For CD and UV absorption spectra of peptides **1** and **3** in chloroform, see also ref 9a.

(34) (a) Nanda, V.; DeGrado, W. F. *J. Am. Chem. Soc.* **2004**, *126*, 14459−14467. (b) Pengo, B.; Formaggio, F.; Crisma, M.; Toniolo, C.; Bonora, G. M.; Broxterman, Q. B.; Kamphuis, J.; Saviano, M.; Iacovino, R.; Rossi, F.; Benedetti, E. *J. Chem. Soc., Perkin Trans. 2* **1998**, 1651−1657.

(35) Phenyl orientations at χ^2 and ($\chi^2 + 180°$) produce the same chemical structure due to the χ^2 symmetry.[22c] Meanwhile, phenyl moieties in the energy-minimized right-handed 3_{10}-helix (Figure 1a) do not retain the strict hexagonal symmetry, thereby generating some energy difference in χ^2 and ($\chi^2 + 180°$). Thus the re-optimization for bond lengths and angles were carried out at each χ^2 point. Within errors caused in the above procedures, $\chi^2 = 0°$ and 180° (or 360°) yielded almost the same results in structures, CD spectra and energies, as shown in Figures 4−7 and SFigure 1.

(36) The χ^2 energy diagram was calculated for a Δ^ZPhe residue incorporated into the midpoint of right-handed 3_{10}-helical $CH_3CO\text{-}Aib_3\text{-}\Delta^Z\text{Phe-}Aib_3\text{-}NHCH_3$. The 3_{10}-helix was energy-minimized from a 3_{10}-helix (−60°, −30°)[20] with $\chi^2 = 40°$ [23] (p-type) by the AM1 method,[16] and then the χ^2-angle rotated from 0° to 350° with a step of 10°. (ϕ, ψ, ω) averaged for the backbone is (−50°, −33°, 180°). At each χ^2 point, all bond lengths and bond angles were re-optimized by the AM1 method.[35] For these conformers, each single-point energy was obtained at the AM1 level in MOPAC97[16] (SFigure 1A) and the B3LYP/6-31G** level in Gaussian 03[13] (SFigure 1B). In both diagrams, similarities between energies of χ^2 and ($\chi^2 + 180°$) seem to reflect the χ^2-symmetry, ensuring essential validity in the energy diagrams. Both diagrams exhibit a barrier of ca. 3 kcal mol^{-1} in full rotation of the χ^2 angle, but the profiles are somewhat different. The AM1-prediction results in the most stable orientation around 50° (p-type orientation), and second-stable around 140°. In contrast, the DFT method predicts the most stable orientation around 160° (essentially, ν-type orientation), and a second-stable slope around 0−30°. Our CD simulation suggesting a preference for ν-type orientations might reflect the DFT-prediciton.

(37) AM1-optimized 3_{10}-helical peptide **2** with the ν-type was also displayed in ref 9h. For conformational analysis of (Δ^ZPhe-Aib)-based peptides, see ref 9. For theoretical conformational studies of $CH_3CO\text{-}(Aib\text{-}\Delta^Z\text{Phe})_m\text{-}NHCH_3$, see also: (a) Nandel, F. S.; Khare, B. *Biopolymers* **2005**, *77*, 63−73.

(38) For comparison of excited states in several MO methods, see refs 3b and 4b,h.

(39) The bandwidth of band I is defined by $(\Delta/2)_L = (\lambda_L - \lambda_{max})$ or $(\Delta/2)_{av} = (\lambda_L - \lambda_S)/2$: λ_{max} is the peak position; λ_L and λ_S are positions at (1/e) height for longer and shorter wavelengths, respectively. Because the λ_S value might be somewhat influenced by partial overlap with absorption bands at higher energy levels, the $(\Delta/2)_L$ is also used. The absorption profile of **1** in chloroform yields $(\Delta/2)_L = 27$ nm and $(\Delta/2)_{av} = 32$ nm. For a similar estimation of Δ from UV absorption profile, see 11b.

(40) In the theoretical CD spectra of Figure 1a, selected combinations of (Δ/2: λ_{12}, amplitude) are as follows [Δ/2 and λ_{12} are in nanometers, and amplitude is $(\Delta\epsilon_{max} - \Delta\epsilon_{min})$ in split CD spectrum]. For the velocity form, (20: 30, 31), (21: 32, 28), (22: 33, 26), and (23: 35, 24); for the length form, (21: 30, 34), (22, 32, 31), (23, 33, 29), and (24: 35, 27). In experimental CD spectra (Figure 3 and SFigure 17), (λ_{12}, amplitude) is estimated: for peptide **1**, (34, 16) in chloroform (Figure 3b), and (29, 15) in tetrahydrofuran; for peptide **3**, (34, 30) in chloroform (SFigure 17b), and (33, 30) in tetrahydrofuran. For interpretation of split CD amplitude and profile, see also ref 11b.

(41) Karelson, M. M.; Zerner, M. C. *J. Phys. Chem.* **1992**, *96*, 6949−6957.

(42) Inai, Y.; Ousaka, N.; Miwa, Y. *Polym. J.* **2006**, *38*, 432−441.